Power management and control strategies for efficient operation of a solar power dominated hybrid DC microgrid for remote power applications

Citation:
Mendis, N., Mahmud, M. A., Roy, T. K., Haque, M. E. and Muttaqi, K. 2016, Power management and control strategies for efficient operation of a solar power dominated hybrid DC microgrid for remote power applications, *in IACC 2016 : Proceedings of the 51st IEEE IAS Industrial Automation and Control Committee Annual Meeting*, IEEE, Piscataway, N. J., pp. 1-8.

DOI: http://dx.doi.org/10.1109/IAS.2016.7731816

Power Management and Control Strategies for Efficient Operation of a Solar Power Dominated Hybrid DC Microgrid for Remote Power Applications

N. Mendis *Member, IEEE*, M. A. Mahmud, *Member, IEEE*, T. K. Roy, *Student Member, IEEE*, M. E. Haque, *Senior Member, IEEE*, and K. M. Muttaqi, *Senior Member, IEEE*

***Abstract*—In this paper, a hybrid DC microgrid consisting of a diesel generator with a rectifier, a solar photovoltaic (PV) system, and a battery energy storage system is presented in relation to an effective power management strategy and different control techniques are adopted to power electronic interfaces. The solar PV and battery energy storage systems are considered as the main sources of energy sources that supply the load demand on a daily basis whereas the diesel generator is used as a backup for the emergency operation of the microgrid. All system components are connected to a common DC bus through an appropriate power electronics devices (e.g., rectifier systems, DC/DC converter). Also a detailed sizing philosophy of all components along with the energy management strategy is proposed. Energy distribution pattern of each individual component has been conducted based on the monthly basis along with a power management algorithm. The power delivered by the solar PV system and diesel generator is controlled via DC-DC converter and excitation controllers which are designed based on a linear quadratic regulator (LQR) technique as as proportional integral (PI) controllers. The component level power distribution is investigated using these controllers under fluctuating load and solar irradiation conditions and comparative results are presented.**

***Index Terms*—DC microgrid, solar PV system, diesel generator, battery energy storage system, sizing of components, energy management.**

I. Introduction

DC microgrids are used to satisfy to the load demand of remote locations such as telecommunication and railway sites. Such microgrids generally consist of a diesel generator, a battery energy storage system, and a renewable energy source to perform the hybrid operation. In most of the cases, solar photovoltaic (PV) systems are considered as the preferred source of renewable energy for a DC microgrid due to several advantages such as less capital cost for environmental conditions (i.e., open areas leading to high sun density) and low complexities associated with the structural requirements.

Most of the remote locations are very difficult to reach and thus, the continuous supply of fuel is not continuously available. The operation of diesel generators mainly depends on the availability of fuel and therefore, its role is limited as a backup/emergency supply [1]. The battery energy storage system (BESS) is considered as one of the most reliable sources of energy as it can be charged either via a solar scheme or a diesel generator. However, the size of the battery storage system plays a significant role in determining the overall capital cost of a DC microgrid system as well as the autonomy of operation. Therefore, the selection of the battery storage capacity should be made to have an optimize cost while maintaining the reliability of operation [2]–[4].

Industry standard DC power system can be designed to supply the DC loads with 12 V, 24 V, 48 V, 110 V or even higher. If the load requires different output voltage levels, then suitable DC/DC conversion can be employed to achieve the appropriate voltage levels. However, such a DC/DC conversion can lead to a single point of failure. There are several factors should be considered when designing a microgrid systems. One of the most important critical design inputs is the load analysis of the remote site, autonomy time for the battery storage, and diesel fuel tank, shading effect and wind loading factors for solar, etc. [5]–[7]. Most of the above stated information can be directly obtained by having a site visit or through the consultation of the respective personnel. There are several power electronic interfaces involved with the operation of DC microgrids. All the major energy sources (i.e. solar PV, diesel generator and battery storage systems) are connected to a common DC bus through rectifiers and/or regulators. In this regard, redundancies of the components (e.g., N+1) and their reliability of operation are para important. Also, proper protection schemes (e.g., over voltage, transient over voltage, low voltage battery disconnection, etc.) should be incorporated to the DC microgrid considering many design aspects as such as coordinated discrimination [8].

The energy management of DC microgrids is another important challenge as the overall operational efficiency depends on the power sharing capability of the system components [9]. In DC microgrids, the voltage at the common DC bus is important that needs to be maintained at a constant value as the stability of the whole system depends on the DC bus voltage [10]–[12]. The DC bus voltage is regulated based on the power balance of the microgrid system. However, the maintenance of power balance is a challenging task as it requires detailed control design for the power electronic interfaces [13]–[15].

This paper aims to provide a detailed analysis of a commercial hybrid DC microgrid which can be widely adopted by telecommunication and railway industries. An analytical framework is proposed for the sizing of different components of the DC microgrids. Moreover, the excitation system and rectifiers of the diesel generator along with DC-DC converter is controlled by using linear quadratic regulator (LQR) controller and different possible operational modes of the DC microgrid are considered. The performance the performance of the proposed controller is evaluated against a traditional proportional integral (PI) controller.

N. Mendis is with the Eltek Australia Pty Ltd, Port Melbourne, VIC 3207, Australia. Email: nnrm786@uowmail.edu.au

M. A. Mahmud, T. K. Roy, and M. E. Haque are with the School of Engineering, Deakin University, Waurn Ponds, VIC 3216, Australia. Email: (apel.mahmud, tkroy, and enamul.haque)@deakin.edu.au

K. M. Muttaqi is with the School of Electrical, Computer and Telecommunications Engineering, University of Wollongong, NSW 2522, Australia. Email: Kashem@uow.edu.au

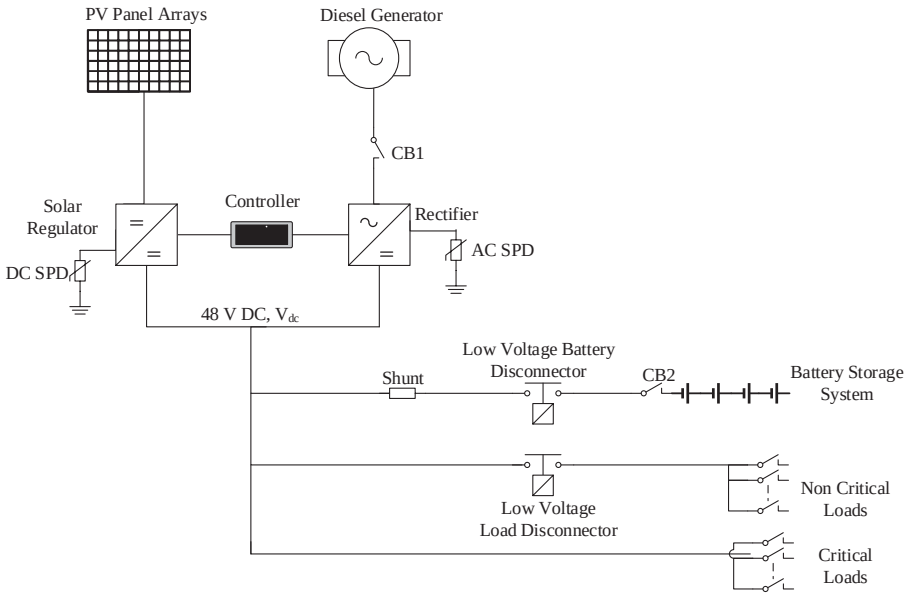

Fig. 1. A commercial hybrid DC microgrid system

Simulations are conducted to justify the analytical framework for sizing and power management with the proposed controllers under different operating conditions.

The paper is organized as follows. Section II includes the overview of a commercial DC microgrid. Section III is presenting the analytical framework for the sizing of different components such as loads, solar PV systems, BESSs, and diesel generators. Section IV represents the hybrid operation of the DC microgrids and Section V-A presents the controller design techniques while Section VI provides the relevant simulation results. Finally, Section VII summarizes the main outcomes and scopes for the future works.

II. Structure of a Commercial DC Microgrid

In this paper, a commercial hybrid DC microgrid that can be employed for telecom and railway power applications is considered. The microgrid is consisting of the following main components:

1) a diesel generator with a rectifier,
2) a solar PV system with a DC-DC converter (solar regulator),
3) a BESS which directly connected to the DC bus, and
4) DC loads (critical and noncritical)

The proposed hybrid DC microgrid is shown in Fig. 1 from where it can be seen that all components (except DC loads or the BESS) are connected to the DC bus either via DC-DC converters (e.g., solar PV system via a solar regulator) or via the rectifier (e.g., the diesel generator).

The DC loads can be connected directly to the DC bus if the rated voltage of the loads is similar to that of the DC bus. However, a DC-DC buck or boost converter is required to connect the DC loads if a different voltage is required than the DC bus voltage, V_{dc}. The component sizing and practical design are considered as the key elements of the design process of a DC microgrid and they are discussed in the following section.

III. Sizing and Practical Design Considerations

This section is intended to illustrate the components sizing associated with DC microgrid depicted in Fig. 1. There are many factors which influence the sizing of different components in a microgrid. Among these factors, the overall costs (capital and operating) and reliability of the supply are considered to be predominant elements. Some designs may be cost competitive while trade off other important features such as the autonomy time (i.e., the continuity of the supply). The sizing of different components in the commercial hybrid DC microgrid which is used in this paper is illustrated below:

A. Sizing of Loads

The DC load demand of the existing equipment is generally provided by the client of the project. The DC load mainly corresponds to the customer load component ($P_{L_{site}}$) used to supply the site equipment (e.g., signaling device). However, additional DC loads, due to the presence of cubicles ($P_{L_{cubicle}}$) should be taken into consideration. For example, most of the batteries used in microgrid environments are placed in IP5X or IP6X rated cubicles that consist of cooling (e.g., fan, heat exchanger or DC air conditioner, control units power supply). Therefore, the DC power consumption associated with the cooling system should be considered. In some situations, the extra power requirement (i.e., $P_{L_{cubicle}}$) can be greater than the actual site load requirement ($P_{L_{site}}$). The total load of the site can be calculated as in equation (1).

$$P_{L_{total}} = P_{L_{site}} + P_{L_{cubicle}} \tag{1}$$

where $P_{L_{total}}$ is the total power for the designed microgrid, $P_{L_{site}}$ is the power consumed by the site loads, and $P_{L_{cubicle}}$ is the additional load requirement due to the presence of cubicles (cooling, charger control supply, etc.).

B. Sizing of BESS

The BESS can be considered as the most critical component of the proposed DC microgrid. The autonomy or continuous running time of the microgrid system mainly depends on the capacity of the BESS. In general, the autonomy time of the battery storage system for a microgrid can be 3 to 7 days. However, longer

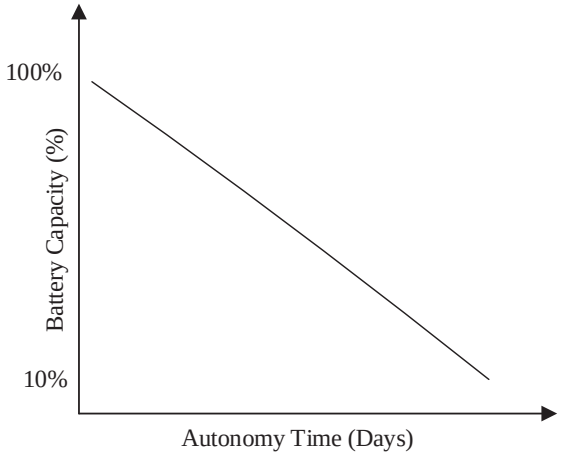

Fig. 2. Battery capacity over autonomy time (It is assumed that battery is being discharged following linear characteristics)

running time means the higher cost and therefore, the size of the BESS should be selected carefully. The depth of discharge (DOD) is one of the key parameters for sizing the BESS. If the battery is charged to 100% of its capacity defined by $\%C_{battery}$ and the autonomy time is $t_{autonomy}$ (e.g., 7 days), then the DOD of the battery can be written as follows:

$$DOD_{battery} = \frac{\%C_{battery}}{t_{autonomy}} \tag{2}$$

where $DOD_{battery}$ is the DOD for the battery, $\%C_{battery}$ is the percentage capacity of the battery, and $t_{autonomy}$ is the time to maintain the continuity of the supply through the battery. The DOD for the battery ($DOD_{battery}$) decreases with the increase in the time for the autonomy ($t_{autonomy}$) which is illustrated in Fig. 2.

The ampere-hour (Ah) capacity of the battery can easily be calculated if the following items are known:

- load voltage,
- total power of the load,
- design margin (DM),
- time for autonomy,
- the DOD,
- aging factor (AF), and
- temperature compensation factor (TC).

Based on above factors, the capacity of the battery can be given as in equation (3).

$$C_{battery}(\text{Ah}) = \frac{P_{L_{total}} \times t_{autonomy} \times DM \times AF \times TC}{DOD_{battery} \times V_{load}} \tag{3}$$

where $C_{battery}$ is the capacity of the battery in Ah, DM, AF, and TC are the design margin, aging factor, temperature compensation factor, respectively, and V_{load} is the load voltage. It is to be noted the total power consumed by the load ($P_{L_{total}}$) should be provided in Watt (W).

C. Sizing of Solar PV System

The size of the required solar panels depends on many factors such as shading, albedo setting, etc. However, a detailed analysis of these factors has not been included in this paper. The sizing of the panels is mainly determined by considering the insolation levels of each month where the insolation level for a year is shown in Fig. 3 and the designed total load ($P_{L_{total}}$) of the site. The effective area of the solar panel is a measure of area that solar panels should have under the standard operating condition (irradiance, $s = 1000$ W/m^2, temperature, $T = 25^o$C, and air mass, $AM = 1.2$) can be calculated as follows:

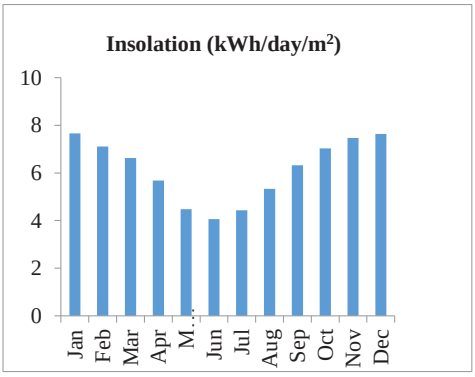

Fig. 3. Insolation level of the site location

$$A_{eff}(\text{Panel}) = \frac{P_{rated}(\text{Panel})}{s \times \eta(\text{Panel})} \tag{4}$$

where A_{eff}(Panel) is the effective area of the solar panel, P_{rated}Panel is the solar panel rating in Watts, s irradiance at standard conditions, and ηPanel is the efficiency of the solar panel.

The number of panels, N_{Panels} required based the lowest irradiance level on the monthly basis (In this case, the lowest irradiance level is in June as shown in Fig. 3) can be determined by the following equation:

$$N_{Panels} = \frac{P_{L_{total}} \times 24}{I_{lowest} \times A_{eff}(\text{Panel} \times \eta_{panel} \times \eta_{regulator}} \tag{5}$$

where I_{lowest} is the insolation level at the lowest month (kWh/day/m^2), η_{panel} is the efficiency of the solar panel, and $\eta_{regulator}$ is the efficiency of the solar regulator.

D. Sizing of Diesel Generator

In this paper, the sizing of the diesel generator is estimated by considering two parameters: (a) total design load ($P_{L_{total}}$) and (b) charging rate of the battery (typically C_8 or C_{10}). Therefore, the size of the diesel generator can be calculated as follows:

$$P_{Generator} = P_{L_{total}} + \frac{C_{battery}(\text{Ah})}{(\text{Charging rate})} \times V_{load} \tag{6}$$

IV. Hybrid Operation of DC Microgrids

The operating modes of the hybrid DC microgrids depends on the load demand, available capacity of the BESS, power output from the solar PV system, and power supplied by the diesel generator. There are several uncertainties associated with the operational performance of the microgrid system: (a) varying load and (b) fluctuating weather conditions. Therefore, controllers are required to regulate the output power of all components with a view to maintain the power balance. In this regard, the DC bus voltage, V_{dc} is taken as the desired control objective. The power balance equation of the hybrid DC microgrid system depicted in Fig. 5 can be written as in equation (7):

$$P_{Generator} + P_{pv} \pm P_{battery} = P_{L_{total}} \tag{7}$$

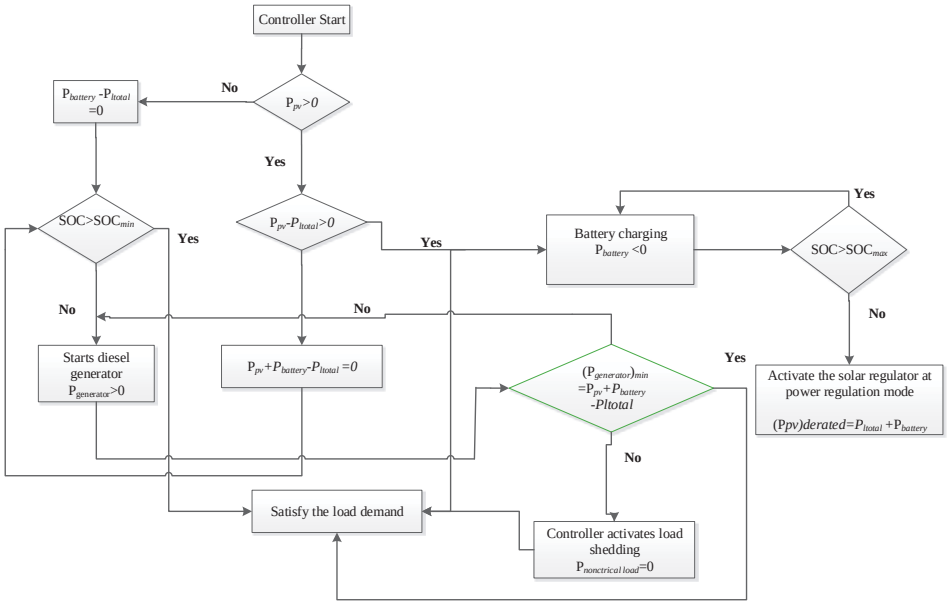

Fig. 4. Power management strategy of the microgrid system

where P_{pv} is the output power of the solar PV system, and $P_{battery}$ is the power available from the battery. The '$\pm$' sign is used for $P_{battery}$ battery can supply power or store energy, i.e., it allows discharging and charging, respectively.

The output power of the solar PV system is fluctuating and therefore, a solar regulator is used to supply the power into the DC bus where the loads are connected. In the DC microgrid, the power available from the solar PV system is utilized either by supplying the load or by storing excessive energy into the BESS. Therefore, it is essential to control the solar regulator in a manner that it does not operate outside the specified limits of DC bus voltage. For example, the solar regulator should have specified input voltage and power limits that need to be taken into consideration. The power limits of a solar also determine the number of panels that can be connected to a regulator. These voltage and power limits can be written as follows:

$$\begin{cases} (V_{\text{regulator}})_{\text{min}} < V_{\text{regulator}} < (V_{\text{regulator}})_{\text{max}} \\ (P_{\text{regulator}})_{\text{min}} < P_{\text{regulator}} < (P_{\text{regulator}})_{\text{max}} \end{cases} \tag{8}$$

where $V_{\text{regulator}}$ is the operating voltage of the regulator, $P_{\text{regulator}}$ is the operating power of the regulator, and the subscripts min and max correspond the minimum and maximum values of the respective variables.

The role of the BESS in a hybrid DC microgrid is to supply the load when the solar PV systems do not generate sufficient power to match the load demand. It is to be noted that the availability of the battery storage system is subjected to following condition:

$$SOC_{min} < SOC \leq SOC_{max} \tag{9}$$

where SOC is the state of charge of the battery, SOC_{min} is the minimum limits of the SOC, and SOC_{max} is the maximum limits of the SOC.

The diesel generator is controlled to supply power when there is no power from the solar PV system as well as the energy stored into the BESS is not sufficient to deliver the loads. The output power of the diesel generator is usually controlled through the governor-excitation system. A rectifier system (AC/DC conversion) should be incorporated to interface the diesel generator with the DC bus. However, the power output of the diesel generator should meet the minimum power requirement $(P_{Generator})_{min}$ to avoid operating at lower efficiency. Typically the the minimum loading of the diesel generator should be 30% of its rated power output. If this condition is not met, the load shedding scheme should be employed. Non-critical loads can be connected via low voltage load disconnector as shown in Fig. 1 which can be activated via a controller. The control operation of each component is based on the power management scheme as depicted in Fig. 4.

In this paper, the controllers for the converter of the solar PV system and the excitation system of the diesel generator are designed by using a linear quadratic regulator (LQR) approach as discussed in the following section.

V. Controller Design

The controllers are designed based on the dynamic model of the diesel generator and solar PV system. The diesel generator in the microgrid is mainly a synchronous generator and the excitation system of the synchronous generator can be controlled to control the terminal voltage of the synchronous generator which in turn control the output power. Similarly, the output power of the solar PV system can be controlled by controlling the DC-DC converter. The dynamical models of the diesel generator and solar PV system along with the controller design technique are discussed in following subsections:

A. Dynamical Models of the Diesel Generator and Solar PV System

The diesel generator is a synchronous generator and its dynamical model is used to design the excitation controller. A synchronous generator can be represented in different ways based on its intended applications. In this paper, the one-axis model of the synchronous generator is used along with the dynamics of the excitation system. The one-axis model of a synchronous generator along with the mechanical dynamics can be written as

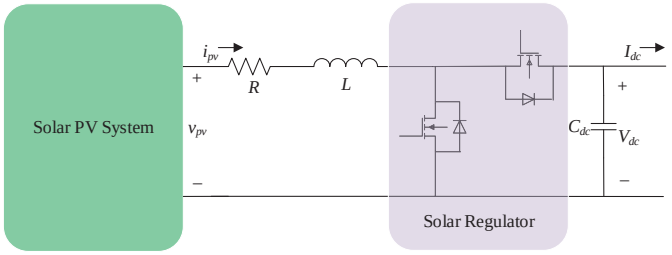

Fig. 5. Solar PV system with a solar regulator (DC-DC buck-boost converter)

follows [16]:

$$\begin{aligned}\dot{\delta} &= \omega - \omega_0 \\ \dot{\omega} &= -\frac{D}{2H}(\omega - \omega_0) + \frac{\omega_0}{2H}(P_m - P_e) \\ \dot{E}'_q &= -\frac{1}{T'_{do}}E'_q - \frac{(x_d - x'_d)}{T'_{do}}I_d + \frac{1}{T'_{do}}E_{fd}\end{aligned} \tag{10}$$

where δ is the rotor angle, ω is the operating speed, ω_0 is the synchronous speed, D is the damping coefficient, H is the inertia constant, P_m is the mechanical power input, and P_e is the electrical power output of the synchronous generator, E'_q is the field variable proportional to field flux linkages, T'_{do} is the d-axis transient open-circuit time constant, x_d is the d-axis synchronous reactance, x'_d is the d-axis transient reactance, I_d is the d-axis current component, and E_{fd} is the equivalent field excitation voltage.

The excitation system is considered as an IEEE Type II exciter whose dynamics can be written as [17]:

$$\dot{E}_{fd} = -\frac{E_{fd}}{T_A} + \frac{K_A}{T_A}(V_{ref} + V_c - V_t) \tag{11}$$

where T_A is the time constant of the voltage regulator, K_A is the gain of the voltage regulator, V_{ref} is the reference terminal voltage, V_c is the stabilizing signal which is control input of the system.

The terminal voltage of the synchronous generator can be written as follows:

$$V_t = \sqrt{\left(E'_q - x'_d I_d\right)^2 + \left(x'_d I_q\right)^2} \tag{12}$$

Since a rectifier is used to convert AC power into DC power, the conversion dynamics can be written as

$$V_t = m_r V_{dc} \tag{13}$$

where m_r is the modulation index of the rectifier which is another control input and V_{dc} is the DC bus voltage of the microgrid which is the output of the system.

For the solar PV system, the solar regulator is considered as a DC-DC buck-boost converter is used and the block diagram representation of a solar PV system with a solar regulator is shown in Fig. 5. The dynamical model of the solar PV system with a solar regulator can be written as follows:

$$\begin{aligned}\dot{i}_{pv} &= \frac{1}{L}\left(v_{pv} - Ri_{pv} - m_c V_{dc}\right) \\ \dot{V}_{dc} &= \frac{1}{C}\left[(1 - m_c)i_{pv} - I_{dc}\right]\end{aligned} \tag{14}$$

where i_{pv} is the output current of the solar PV system, v_{pv} is the output voltage of the solar PV system, R is the combination of internal resistances of solar cells as well as the connecting lines, L is the inductance of the lines, C_{dc} is the output capacitance of the DC-DC converter, I_{dc} is the output voltage, m_c is the control input for the DC-DC converter, and the control objective is the DC bus voltage (V_{dc}). The controllers are designed based on these dynamical models of the diesel generator and solar PV system and the detailed design procedure for designing a LQR controller is discussed in the following subsection.

B. LQR Controller Design

The dynamical model of the diesel generator and solar PV system can be written in the following form of the generalized linear system:

$$\begin{aligned}\dot{\mathbf{x}} &= \mathbf{A}\mathbf{x} + \mathbf{B}\mathbf{u} \\ \mathbf{y} &= \mathbf{C}\mathbf{x}\end{aligned} \tag{15}$$

where the symbols have their usual meanings. For the diesel generator, the states (**x**) are δ, ω, E'_q, and E_{fd}. Similarly, the states for the solar PV system is i_{pv} and V_{dc}. The control input (**u**) for the excitation system is V_c and the rectifier is m_r while that of for the DC-DC converter is m_c. In both cases, the control objective is the same which is the DC bus voltage.

In order to design the LQR controller, the linear quadratic performance index is usually chosen with the conditions $x(t_0) = x_o$ and $x(\infty) = 0$ as [18]:

$$\mathbf{J}(\mathbf{x}, \mathbf{u}, \mathbf{Q}, \mathbf{R}) = \int_0^\infty (\mathbf{x}^T\mathbf{Q}\mathbf{x} + \mathbf{u}^T\mathbf{R}\mathbf{u})\,\mathrm{d}t \tag{16}$$

where **Q** is a semi- or positive definite weighting matrix and **R** is a real symmetric positive definite weighting matrix. In LQR design, the **Q** and **R** matrices are in such a way that $\mathbf{Q}^T \geq \mathbf{Q}$ and $\mathbf{R}^T > 0$ which determine the relationship between the error and the expenditure of energy rate. The objective of the linear quadratic regulation is to find the optimal control law in such a manner that the system is stable and **J** is minimized. The optimal control law can be written as follows:

$$\mathbf{u} = -\mathbf{K}\mathbf{x} \tag{17}$$

The optimal gain matrix **K** can be calculated as follows:

$$\mathbf{K} = \mathbf{R}^{-1}\mathbf{B}^T\mathbf{P} \tag{18}$$

where **P** is a positive definite which is the unique solution of the following Riccati equation:

$$\mathbf{A}^T\mathbf{P} + \mathbf{P}\mathbf{A} - \mathbf{P}\mathbf{B}\mathbf{R}^{-1}\mathbf{B}^T\mathbf{P} + \mathbf{Q} = 0 \tag{19}$$

The control laws for the diesel generator with the excitation system and rectifier can be obtained by using equation (17). The implementation block diagram for the excitation controller of a diesel generator along with a rectifier and the controller for the solar regulator are shown in Fig. 6. The performance of the LQR controller is compared with a PI controller and an overview of the PI controller is provided in the following subsection.

C. Overview of PI Controller

Fig. 7 represents the basic block diagram representation of a PI controller which is used for the hybrid operation of the DC microgrid. From Fig. 5, it can be seen that the desired voltage of the DC bus is considered as the reference voltage (V_{dcref}) for the first PI controller and to generate the reference value of the current (I_{dcref}). This current is used to control the output the DC power which can be written as follows:

$$P_{dc} = V_{dc}I \tag{20}$$

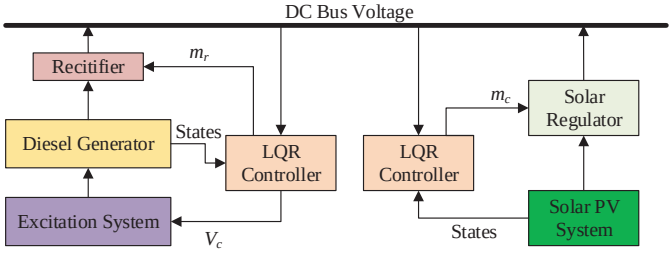

Fig. 6. Block diagram: implementation of LQR controllers for diesel generator and solar PV system

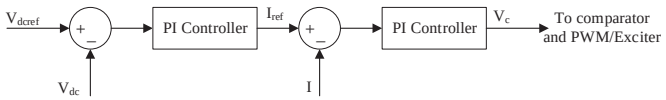

Fig. 7. Block diagram: implementation of PI controllers for diesel generator and solar PV system

where P_{dc} is the output power of the component which is delivering power to the load and I is the output current of that particular component. Also, the control operation of each component is based on the power management scheme as depicted in Fig. 4.

Computer simulations are carried out in the following section to validate the sizing and hybrid operation of the DC microgrid along with the implementation of the proposed controllers.

VI. Results

The performance of the proposed commercial hybrid DC microgrid shown in Fig. 1 is investigated by considering two main points: a) the sizing philosophy as discussed in Section III and on the basis of monthly energy distribution and b) the operational strategy as discussed in Section IV. These have been discussed in the following two subsections:

A. Validation of Sizing Philosophy

As mentioned earlier, the microgrid system comprises of a diesel generator, a solar PV system, a BESS, and loads. The sizing of these components are done by considering the formulas as presented in Section III and listed in Table I.

Different operational conditions are considered. In this regard, the operation of the DC microgrid with different solar panel sizing, diesel generator and battery storage have been investigated. Following assumptions have been considered when analyzing the monthly energy distribution:

1) Solar irradiation is constant throughout the month and the effective solar period is 4 hours per day

TABLE I
System components & their capacities

Component description	Capacity
Total designed load, $P_{L_{total}}$	480 W at 48 V DC
No. of solar panels, N_{panels}	24, 60, & 6 for Case I, II, & III
Rating of solar panel, P_{panel}	260 W
Autonomy time, $t_{autonomy}$	3 days
Battery energy storage capacity, $C_{battery}$	1320 Ah
Diesel generator rating, $P_{generator}$	14 kVA

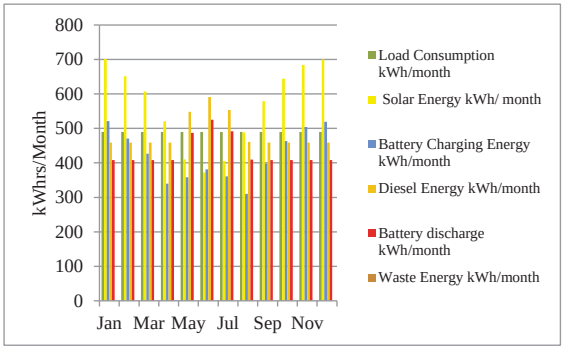

Fig. 8. Energy profile of a commercial hybrid DC microgrid–24 solar panels

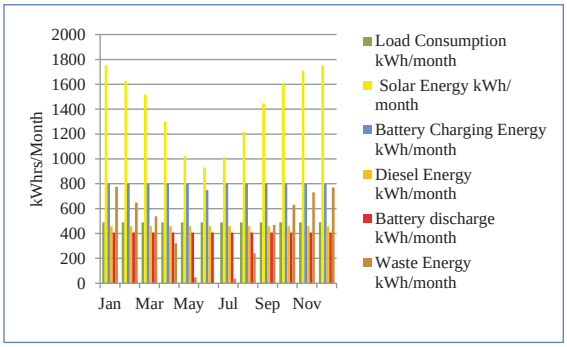

Fig. 9. Energy profile of a commercial hybrid DC microgrid–60 solar panels

2) Battery is supplying energy to the load during the rest of the day
3) If battery capacity drops to 50% of its DOD, the diesel generator is kicked in and supplying the load and charging the battery at C_{10} rate

All simulations are conducted based on the remote location which is having insolation levels as depicted in Fig. 3. Three cases have been chosen based on the selection of different numbers of solar panels.

In the first case, the number of solar panels is selected as 24 which is considered as an ideal case for the microgrid which is shown in Fig. 8. There are no energy wastage and maintain the consumption of diesel energy and battery discharge energy at moderate levels. It can be noticed that the highest battery charging energy is exhibited during the month that corresponds to the highest solar energy generation. Also, the battery discharging and diesel energy have been increased during the low solar irradiation months such as in July.

In the second case, 60 solar panels are selected which represents an oversized scenario and the energy profile is shown in Fig. 9. As anticipated, the energy wastage occurs due to the excessive power generation from the solar panels. As stated above, under practical situation such excessive or wasted energy will be controlled via the solar regulator. Also, it can also be seen that there is an increase in battery charging energy due to the availability of high power generation from the solar panels resulting a reduced contribution from the diesel generator.

The third case represents an undersized solar requirement and the energy distribution is shown in Fig. 10. It can be noted that, the battery charging energy has been reduced as compared to

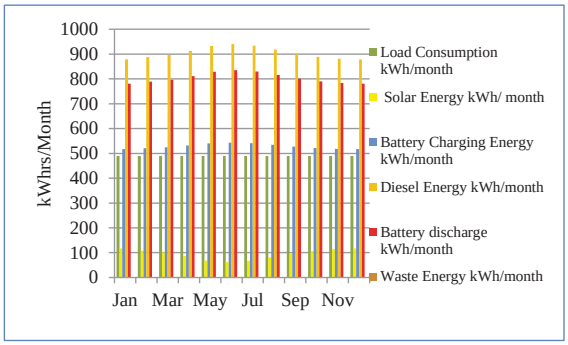

Fig. 10. Energy profile of a commercial hybrid DC microgrid–6 solar panels

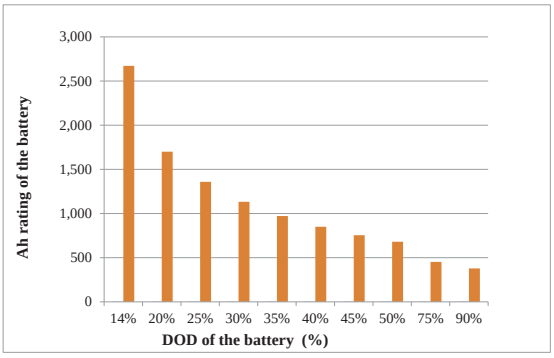

Fig. 11. DOD of the battery storage system

previous two cases. Also, the energy component corresponds to the battery discharging is increased due to the reduced solar generation. Similarly, the diesel generation has been increased significantly compared to the first two cases.

Fig. 11 shows the DOD of the battery with the estimated capacity. In this paper, the autonomy time for the battery is taken as 3 days which corresponds to 30% DOD/day. Also it is evident from Fig. 11 that the lower DOD increases with the size of the battery storage system.

The operational strategy of the DC microgrid is discussed in the following subsection.

B. Operational strategy and performance evaluation of the controller

In first case, it has been assumed that the solar PV system is operating under standard atmospheric conditions with a solar irradiance of 1000 W/m^2 and environmental temperature of 298 K for a period of t=0 s to t=4 s. The total output power of the solar PV system is considered as 1200 W. In this case study, a load is considered as constant at 480 W during entire period and directly connected to the DC bus whose voltage is 48 V. Now the PV system is supplying 480 W to the load and the additional 720 W power will be stored into the battery which is depicted in Fig. 12(a) and Fig. 12(c), respectively. The power delivered to the load is shown in Fig. 12(b). Therefore, it can be said that there is an exact power balance from t=0 s to t=4 s. The corresponding voltage profile is shown in Fig. 13. At t=4 s, the solar irradiation changes from 1000 W/m^2 to 700 W/m^2 while the temperature remains constant and the microgrid continues to run with this condition until t=8 s. Thus, the output power of the solar PV system will be reduced from 1200 W to 400 W

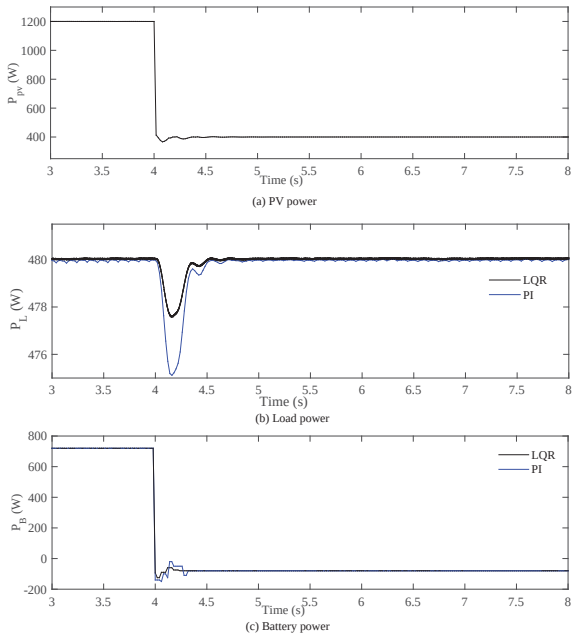

Fig. 12. The output power (a) solar PV system, (b) BESS, and (c) load demand under changing atmospheric conditions

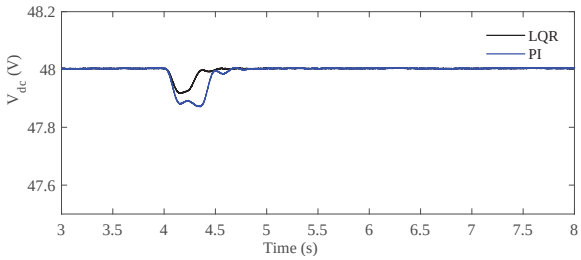

Fig. 13. DC bus voltage under changing atmospheric conditions

from t=4 s to t=8 s as shown in Fig. 12(a). This output power is insufficient to supply the load demand at 480 W and there will be a power shortage of 80 W which will be supplied by the battery as shown in Fig. 12(c). From Fig. 12(b), it can be seen that there are fluctuations of power at the instant t=4 s when the solar irradiation was changing. Moreover, this will also significantly impact the charging rate of the battery and there will be slight variation in the load demand as well as in the DC bus voltage during this period. However, the power balance is obtained immediately due to the power supplied by the BESS. The DC bus voltage exhibits similar characteristics as there are slight variations in this voltage at the instant t=4 s which can be seen from Fig. 13. From these figures, it can be said that the dynamic performance of the designed LQR controller is better than the PI controller.

At the second case, the solar PV system is supplying power to the same load i.e., 480 W with a reduced power output 400 W and the remaining power is being supplied by the BESS. This situation can be considered as the continuation of the previous case where the solar PV system was supplying 400 W power and the BESS was supplying 80 W from t=4 s to t=8 s. Now the DC microgrid continues to run with this condition till t=12 s. At t=12 s, the the following situations are considered:

- the solar PV system is not supplying any power,
- the BESS is fully discharged, and
- the load demand increases from 480 W to 600 W.

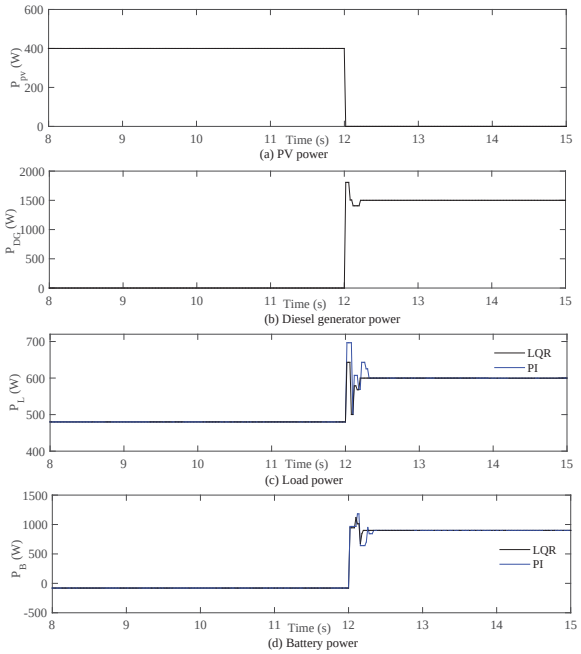

Fig. 14. The output power (a) solar PV system, (b) diesel generator, (c) BESS, and (d) load demand when the diesel generator is in service

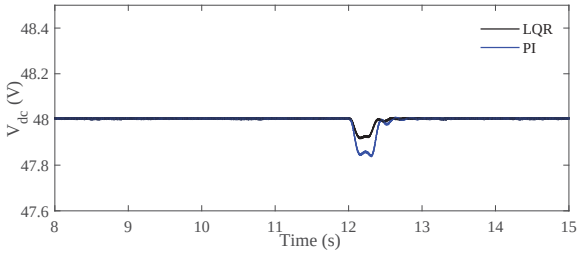

Fig. 15. DC bus voltage when the diesel generator is in service

At t=8 s, these situations have been clearly represented in Fig. 14. In this situation, the only way to supply the power to the load is the diesel generator which is used as a standby generator. In this simulation, the diesel generator is operated to generate an output power of 1500 W. A fraction of this 1500 W will be used to supply the load whose rating is 600 W and the remaining power will be used to charge the BESS. Under such circumstances, the power output profiles for the solar PV system, diesel generator, battery, and load are shown in Fig. 14. During these changes, there will be fluctuations in the DC bus voltage which can be seen from Fig. 15. However, these fluctuations are kept minimum with the designed LQR controller when compared to the PI controller.

VII. Conclusion

In this paper, a solar PV dominated hybrid DC microgrid has been explored whose applications are mainly considered for telecommunication and rail industries. The investigation is conducted by considering all basic components of an industrial and commercial DC microgrid while emphasizing the importance of the proper sizing as well as power management scheme and different control strategies. Monthly energy distribution presented and system level performance also presented under variable load and solar conditions. From the analysis, it has been identified that the appropriate sizing of microgrid component for the cost-effective operations as there will be excess energy due to over sizing while there will be lack of energy due to the under sizing of these components which have been justified based on the data of a remote area. Moreover, the appropriate sizing of the components also ensure a stable dynamic operation of DC microgrid which have been justified through the design of LQR controllers and dynamic simulations under different operating scenarios. Comparative results are presented to demonstrate the performance of the LQR controllers over the traditional PI controllers and these results indicate the superiority of the LQR controllers. Future work will deal with the incorporation of an AC microgrid to supply the local communities in the remote area along with telecommunication and rail industries.

References

[1] C. Nayar, M. Tang, and W. Suponthana, "Wind/PV/diesel micro grid system implemented in remote islands in the Republic of Maldives," *IEEE International Conference on Sustainable Energy Technologies*, pp. 1076–1080, 2008.

[2] L. A. de Souza Ribeiro, O. R. Saavedra, and J. G. de Lima, S. L. abd de Matos, "Isolated micro-grids with renewable hybrid generation: The case of Lenis island," *IEEE Trans. on Sustain. Energy*, vol. 2, no. 1, pp. 1–11, January 2011.

[3] C. Abbey and G. Jos, "A stochastic optimization approach to rating of energy storage systems in wind-diesel isolated grids," *IEEE Trans. on Power Syst.*, vol. 24, no. 2, pp. 418–426, February 2009.

[4] Y. V. Makarov, P. Du, M. C. W. Kintner-Meyer, and H. F. Illian, "Sizing energy storage to accommodate high penetration of variable energy resources," *IEEE Trans. on Sustainable Energy*, vol. 3, no. 1, pp. 34–40, January 2012.

[5] D. Salomonsson and A. Sannino, "Low-voltage DC distribution system for commercial power systems with sensitive electronic loads," *IEEE Trans. on Power Delivery*, vol. 22, no. 3, pp. 1620–1627, July 2007.

[6] B. Wang, M. Sechilariu, and F. Locment, "Intelligent DC microgrid with smart grid communications: Control strategy consideration and design," *IEEE Trans. on Smart Grid*, vol. 3, no. 4, pp. 2148–2156, December 2012.

[7] R. S. Balog, W. W. Weaver, and P. T. Krein, "The load as an energy asset in a distributed DC smartgrid architecture," *IEEE Trans. on Smart Grid*, vol. 3, no. 1, pp. 253–260, March 2012.

[8] D. Salomonsson, L. Soder, and A. Sannino, "Protection of low-voltage DC microgrids," *IEEE Trans. on Power Delivery*, vol. 24, no. 3, pp. 1045–1053, July 2009.

[9] A. T. Elsayed, A. A. Mohamed, and O. A. Mohamed, "DC microgrids and distribution systems: An overview," *Electric Power Systems Research*, vol. 119, pp. 407–417, 2015.

[10] N. L. Diaz, T. Dragicevic, J. C. Vasquez, and J. M. Guerrero, "Intelligent distributed generation and storage units for DC microgridsA new concept on cooperative control without communications beyond droop control," *IEEE Trans. on Smart Grid*, vol. 5, no. 5, pp. 2476–2485, September 2014.

[11] D. Chen, L. Xu, and L. yao, "DC voltage variation based autonomous control of DC microgrids," *IEEE Trans. on Power Delivery*, vol. 28, no. 2, pp. 637–648, April 2013.

[12] P. Karlsson and J. Svensson, "DC bus voltage control for a distributed power system," *IEEE Trans. on Power Electron.*, vol. 18, no. 6, pp. 1405–1412, November 2003.

[13] S. Anand, B. G. Fernandes, and J. Guerrero, "Distributed control to ensure proportional load sharing and improve voltage regulation in low-voltage DC microgrids," *IEEE Trans. on Power Electron.*, vol. 28, no. 4, pp. 1900–1913, April 2013.

[14] A. M. Dizqah, A. Maheri, K. Busawon, and A. Kamjoo, "A multivariable optimal energy management strategy for standalone DC microgrids," *IEEE Trans. on Power System*, vol. 30, no. 5, pp. 2278–2287, September 2015.

[15] Q. Shafiee, T. Dragievi, J. C. Vasquez, and J. M. Guerrero, "Hierarchical control for multiple DC-microgrids clusters," *IEEE Trans. on Energy Conversion*, vol. 29, no. 4, pp. 922–923, December 2014.

[16] P. Kundur, *Power System Stability and Control*. New York: McGraw-Hill, 1994.

[17] M. A. Pai, P. W. Sauer, and B. C. Lesieutre, "Static and dynamic nonlinear loads and structural stability in power systems," *Proceedings of the IEEE*, vol. 83, no. 11, pp. 1562–1572, 1995.

[18] C. Olalla, R. Leyva, A. E. Aroudi, and I. Queinnec, "Robust LQR control for PWM converters: An LMI approach," *IEEE Transactions on Industrial Electronics*, vol. 56, no. 7, pp. 2548–2558, 2009.